ISSN 1070-3284, Russian Journal of Coordination Chemistry, 2021, Vol. 47, No. 10, pp. 664–669. © Pleiades Publishing, Ltd., 2021.
Russian Text © The Author(s), 2021, published in Koordinatsionnaya Khimiya, 2021, Vol. 47, No. 10, pp. 598–603.

Coordination Polymers of Ni(II) with Thiophene Ligands: Synthesis, Structures, and Magnetic Properties

V. A. Dubskikh[a], A. A. Lysova[a], D. G. Samsonenko[a], A. N. Lavrov[a], D. N. Dybtsev[a], *, and V. P. Fedin[a]

[a] *Nikolaev Institute of Inorganic Chemistry, Siberian Branch, Russian Academy of Sciences, Novosibirsk, 630090 Russia*

**e-mail: dan@niic.nsc.ru*

Received March 15, 2021; revised April 9, 2021; accepted April 12, 2021

Abstract—Two new metal-organic frameworks [Ni(btdc)(bipy)$(H_2O)_2$] (**I**) and [Ni(azobipy)$(H_2O)_4$](btdc) (**II**) (H_2btdc is 2,2'-bithiophene-5,5'-dicarboxylic acid, bipy is 4,4'-bipyridyl, and azobipy is 4,4'-azobipyridyl) are synthesized under the solvatothermal conditions. The structures and compositions of the compounds are determined by single-crystal X-ray structure analysis (CIF files CCDC nos. 2068945 (**I**) and 2068946 (**II**)) and confirmed by X-ray diffraction, elemental, and thermogravimetric analyses and IR spectroscopy. The structure of compound **I** is a rare example for mutual interlacing of the network motifs in two independent directions. Compound **II** is ionic and consists of the alternating cationic $[Ni(azobipy)(H_2O)_4]^{2+}$ and anionic $btdc^{2-}$ fragments. The magnetic susceptibility and effective magnetic moment are measured for compound **I** in a temperature range of 1.77–300 K in the magnetic fields up to 10 kOe. The value of μ_{eff} is 3.08 μ_B at 300 K, which is close to the spin-only value for the isolated high-spin Ni^{2+} ion with $S = 1$ (2.83 μ_B) with allowance for the orbital moment contribution. Weak antiferromagnetic interactions are observed between the Ni^{2+} ions at the temperatures $T < 10$ K.

Keywords: metal-organic frameworks, single-crystal X-ray crystallography, magnetic properties

DOI: 10.1134/S107032842110002X

INTRODUCTION

Interest in the chemistry of metal-organic frameworks (MOF) is increasing in the recent several decades, since compounds of this class have unique functional properties that can be finely tuned due to a combination of various organic ligands and metal ions (or clusters) [1–4]. One of the methods for MOF functionalization is the use of bridging ligands containing the heteroatom, including sulfur atom. Relatively high electron density and polarizability of the sulfur atom were shown to improve the sorption and luminescence properties of such coordination polymers [5–10]. In addition, it seems interesting to study the magnetic properties of the MOF based on these ligands [11] and paramagnetic metal cations, in particular, Ni(II). Only several works in which the magnetic properties of the MOF based on Ni^{2+} ions and thiophene-2,5-dicarboxylic acid (H_2Tdc) are discussed have been published at the moment. Some works [12–14] report on the antiferromagnetic interactions between the Ni^{2+} ions in the thiophene-containing coordination polymers inside the $\{Ni_2\}$ or $\{Ni_3\}$ building blocks, and no long-range magnetic ordering is observed in these compounds. The 1D MOF [Ni(Tdc)$(Pen)_2$] (Pen is 1,3-diaminopropane) with the effective magnetic moment (μ_{eff}) equal to 2.62 μ_B at 300 K was reported [15]. The 3D MOF with isolated nickel atoms was synthesized [16]. A decrease in μ_{eff} at $T < 25$ K indicates antiferromagnetic interactions occurring, in authors' opinion, through the carboxylate ligands. No compounds with longer heterocyclic ligands of the thiophene series with the studied magnetic properties were reported.

In this work, the nickel(II)-containing organic coordination polymers were synthesized for the first time using 2,2'-bithiophene-5,5'-dicarboxylic acid (H_2btdc), their crystal structures were determined, and the magnetic properties were studied.

EXPERIMENTAL

The synthesis of H_2Btdc was carried out according to a described procedure [17]. Other initial substances and solvents were used as commercially available reagents without additional purification.

Synthesis of [Ni(btdc)(bipy)$(H_2O)_2$] (I). A mixture of $Ni(NO_3)_2 \cdot 6H_2O$ (29.1 mg, 0.1 mmol), H_2btdc (25.4 mg, 0.1 mmol), 4,4'-bipyridyl (bipy) (15.6 mg, 0.1 mmol), *N*,*N*-dimethylformamide (DMF) (25 mL), water (2.5 mL), and glacial acetic acid (5.5 μL) was sealed in a Teflon reactor and heated in a steel autoclave at 110°C for 48 h. The formed green crystals were washed with DMF (3 × 5 mL) and dried in air. The yield was 23 mg (46%). The composition

and structure of the product were determined by single-crystal X-ray crystallography (XRD).

IR (ν, cm^{-1}): 3639 w, 3391 br.w, ν_s(O–H); 1609 m, 1547 m (ν_{as}(C=O)), 1512 m γ(C–C); 1435 m, 1414 m, 1372 s ν_s(C=O); 1217 m, 1121 w, 1100 w, 1070 w, 1038 w, 1009 w, 887 w, 814 s, 777 s (δ_{oop}(C–H); 752 w, 733 w, 671 w, 648 m, 633 m, 600 m, 567 m, 519 s, 471 w, 438 m.

For $C_{20}H_{16}N_2O_4S_2Ni$

Anal. calcd., %:	C, 47.7	H, 3.2	N, 5.6
Found, %:	C, 47.4	H, 3.1	N, 5.7

Synthesis of [Ni(azobipy)(H_2O)$_4$](btdc) (II). A mixture of $Ni(NO_3)_2 \cdot 6H_2O$ (58.2 mg, 0.2 mmol), H_2btdc (50.8 mg, 0.2 mmol), 4,4'-azobipyridyl (azobipy) (36.8 mg, 0.2 mmol), DMF (2.5 mL), water (2.5 mL), and glacial acetic acid (22 μL) was sealed in a Teflon reactor and heated in a steel autoclave at 110°C for 48 h. The formed red crystals were washed with DMF (3 × 5 mL) and dried in air. The yield was 108 mg (81%). The composition and structure of the product were determined by XRD.

IR (ν, cm^{-1}): 3291 br.m ν_s(O–H); 1603 m, 1564 s ν_{as}(C=O); 1514 m γ(C–C); 1439 s ν_s(C=O); 1420 m, 1366 s ν_s(C=O); 1225 w, 1190 w, 1117 w, 1038 m, 1038 m, 1022 w, 885 m, 845 m, 827 m, 781 s δ_{oop}(C–H); 696 m, 648 m, 575 s, 554 m, 532 w, 521 w, 498 w, 461 w.

For $C_{20}H_{20}N_4O_8S_2Ni$

Anal. calcd., %:	C, 42.3	H, 3.6	N, 9.9
Found, %:	C, 42.2	H, 3.6	N, 9.9

IR spectra in a range of 4000–400 cm^{-1} were recorded in KBr pellets on a Scimitar FTS 2000 FT-IR spectrometer. Thermogravimetric analysis (TG) was carried out on a NETZSCH TG 209 F1 thermal analyzer with the linear heating of the samples in a He atmosphere at a rate of 10 deg min^{-1}. Elemental analysis was carried out on a VarioMICROcube CHN analyzer. The powder X-ray diffraction analysis (pXRD) data were obtained on a Shimadzu XRD 7000S powder diffractometer (CuK_α radiation, λ = 1.54178 Å (**I**) and CoK_α, λ = 1.78897 Å (**II**)).

The magnetization of the polycrystalline samples was measured on a Quantum Design MPMS-XL SQUID magnetometer in a range of 1.77–300 K in the magnetic fields up to 10 kOe. The temperature dependences of the magnetization ($M(T)$) were measured on heating the sample after cooling either in zero magnetic field, or in a specified magnetic field and also on cooling the sample. In order to determine the paramagnetic component of the molar magnetic susceptibility ($\chi_p(T)$), the temperature-independent diamagnetic contribution (χ_d) and possible magnetization of ferromagnetic microimpurities ($\chi_{FM}(T)$) were estimated and subtracted from the measured values of the total molar susceptibility ($\chi = M/H$). The value of χ_d was calculated using Pascal's additive scheme, and $\chi_{FM}(T)$ if any was determined from the measured isothermal dependences $M(H)$ and $M(T)$ data taken in different magnetic fields. To determine μ_{eff} of Ni^{2+} ions, the paramagnetic susceptibility $\chi_p(T)$ was examined using the Curie–Weiss dependence $\chi_p(T) = N_A\mu_{eff}^2 / 3k_B(T - \theta)$, where N_A and k_B are Avogadro's and Bolztmann number, respectively. The effect of the zero-field splitting of the Ni^{2+} ion levels on the magnetic susceptibility was evaluated using earlier described approaches [18].

XRD. The diffraction data for a single crystal of compound **I** were obtained at 100 K on the BELOK Beamlines of the Kurchatov specialized source of synchrotron radiation at the National Research Center Kurchatov Institute (Moscow, Russia) using an area Rayonix SX165 CCD detector (λ = 0.79313 Å, ω scan mode, increment 1.0°). Integration was performed, an absorption correction was applied, and unit cell parameters were determined using the XDS software [19]. The diffraction data for a single crystal of compound **II** were obtained at 140 K on an Agilent Xcalibur automated diffractometer equipped with an area AtlasS2 detector (graphite monochromator, λ(MoK_α) = 0.71073 Å, ω scan mode, increment 0.25°). Integration was performed, an absorption correction was applied, and unit cell parameters were determined using the CrysAlisPro software [20]. The structures were solved using the SHELXT software [21] and refined by full-matrix least squares in the anisotropic (except for hydrogen atoms) approximation using the SHELXL software [22]. The positions of the hydrogen atoms of the organic ligands were calculated geometrically and refined by the riding model. The crystallographic data and details of diffraction experiments are presented in Table 1. The full tables of interatomic distances and bond angles, atomic coordinates, and atomic displacement parameters were deposited with the Cambridge Crystallographic Data Centre ((CCDC nos. 2068945 (**I**) and 2068946 (**II**); https://www.ccdc.cam. ac.uk/structures/).

RESULTS AND DISCUSSION

Single crystals of compound [Ni(btdc)(bipy)(H_2O)$_2$] (**I**) were obtained by heating $Ni(NO_3)_2 \cdot 6H_2O$, H_2btdc, and bipy in a DMF–water (1 : 1 vol/vol) mixture of solvents with a minor addition of glacial acetic acid at 110°C. According to the XRD data, compound **I** crystallizes in the monoclinic crystal system with the symmetry space group $C2$ with $Z = 6$. The independent part of the structure contains one Ni^{2+} cation, one $btdc^{2-}$ anion, one bipy molecule, and two water molecules. The Ni(1) atom exists in the

Table 1. Crystallographic data and structure refinement parameters for compounds **I** and **II**

Parameter	Value	
	I	**II**
Formula	$C_{20}H_{16}N_2NiO_6S_2$	$C_{20}H_{20}N_4NiO_8S_2$
Formula weight	503.18	567.23
Crystal system	Monoclinic	Monoclinic
Space group	*C*2	*C*2/*c*
a, Å	19.623(3)	6.6198(2)
b, Å	11.197(2)	12.8425(5)
c, Å	14.907(2)	26.0359(8)
α, deg	90	90
β, deg	103.80(3)	93.747(3)
γ, deg	90	90
V, Å^3	3180.8(9)	2208.70(13)
Z	6	4
ρ_{calc}, g/cm^3	1.576	1.706
μ, mm^{-1}	1.548	1.126
F(000)	1548	1168
Crystal size, mm	0.07 × 0.05 × 0.03	0.17 × 0.11 × 0.10
Scan range over θ, deg	1.57–31.00	3.14–28.98
Range of indices *hkl*	$-25 \le h \le 25$, $-14 \le k \le 14$, $-17 \le l \le 19$	$-8 \le h \le 9$, $-9 \le k \le 15$, $-33 \le l \le 32$
Number of measured/independent reflections	23003/7131	5115/2442
R_{int}	0.0299	0.0124
Number of reflections with $I > 2\sigma(I)$	7014	2271
GOOF	1.086	1.050
R-indices ($I > 2\sigma(I)$)	$R_1 = 0.0380$, $wR_2 = 0.1076$	$R_1 = 0.0284$, $wR_2 = 0.0724$
R-indices (for all reflections)	$R_1 = 0.0387$, $wR_2 = 0.1088$	$R_1 = 0.0310$, $wR_2 = 0.0736$
Residual electron density (max/min), e/Å^3	0.566/−0.675	1.562/−0.243

octahedral environment formed by two nitrogen atoms of two bipy ligands in the axial position, two oxygen atoms of two carboxyl groups of two btdc^{2-} ligands, and two oxygen atoms of the coordinated water molecules in the equatorial positions (Fig. 1a). The coordination number for the Ni(1) cation is 6. The Ni–N bond lengths are 2.069(6) and 2.090(6) Å, and the Ni–O bonds range from 2.043(3) to 2.086(3) Å. Each nickel(II) cation is linked with four other cations through two bridging bipy molecules and two bridging btdc^{2-} anions, resulting in the formation of 2D network structures (Fig. 1b) with the square topology and cell sizes of 7 × 9 Å. The distances between the planes of the adjacent parallel networks correspond to ~9.7 Å. Interestingly, these networks are arranged in three different orientations parallel to the *c* axis, resulting in the mutual interlacing of all networks of the MOF to form a supramolecular carcass (Fig. 1c). Thus, the crystal structure of compound **I** based on the layered motifs cannot be decomposed without chemical bond cleavage and represents 3D polycatenane. It should be mentioned that the mutual intergrowth according to the polycatenane type is met rather rarely in layered MOF and is interesting from the point of view of target design of coordination and supramolecular compounds [23–25].

Compound [Ni(azobipy)$(H_2O)_4$](btdc) (**II**) was synthesized by heating an equimolar mixture of $Ni(NO_3)_2 \cdot 6H_2O$, H_2btdc, and azobipy in a DMF–water (1 : 1 vol/vol) mixture of solvents with a minor addition of glacial acetic acid at 110°C. According to the XRD data, compound **II** crystallizes in the monoclinic crystal system with the symmetry space group *C*2/*c* with $Z = 4$. The independent part of the structure contains one Ni^{2+} cation, one azobipy molecule, four water molecules, and one btdc^{2-} anion (Fig. 2a). The Ni(1) atom exists in the environment formed by two nitrogen atoms of two azobipy ligands in the axial

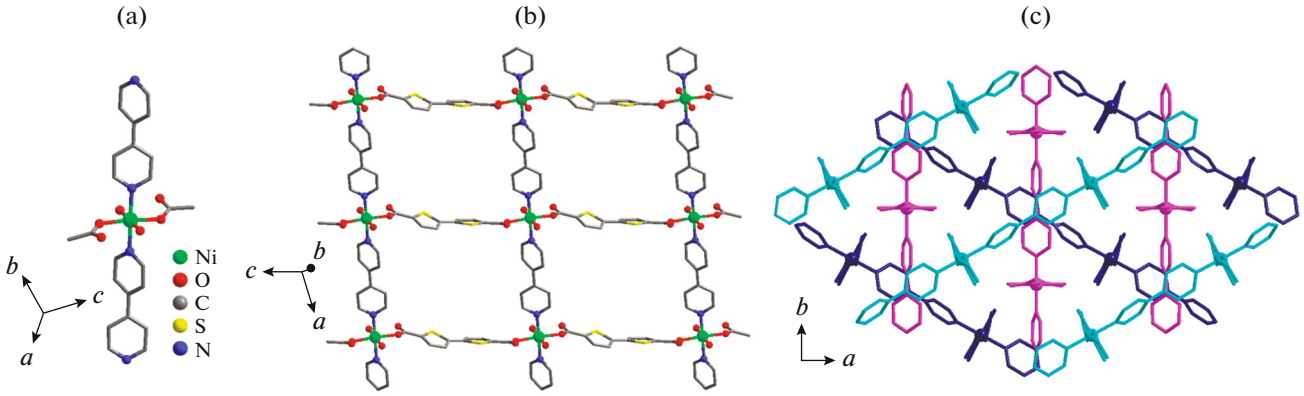

Fig. 1. Structure of MOF **I**: (a) structure of the secondary building block, (b) fragment of the layer, and (c) scheme of mutual interlacing of the coordination networks in the supramolecular carcass structure. Hydrogen atoms are omitted for clarity.

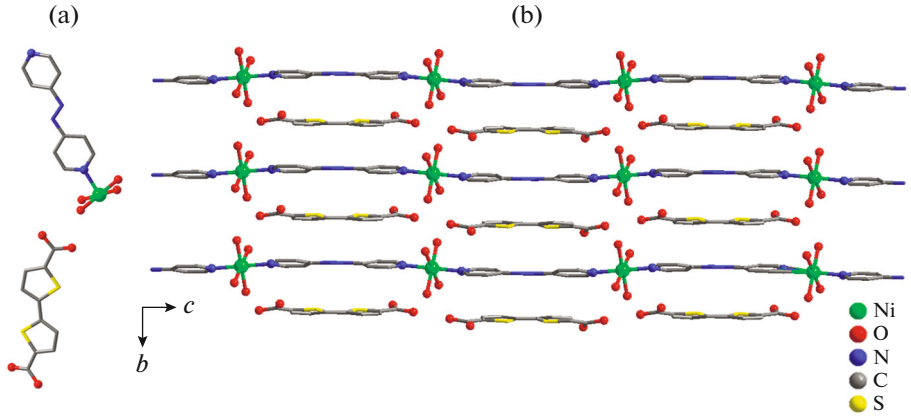

Fig. 2. Structure of MOF **II**: (a) structure of the independent part and (b) view of the crystal packing.

positions and four oxygen atoms of four coordinated water molecules in the equatorial positions. The coordination number of the Ni(1) cation is 6, and the coordination polyhedron is an octahedron. The Ni–N bond lengths are 2.0971(15) and 2.0972(15) Å, and the Ni–O bonds range from 2.0443(13) to 2.1144(13) Å. The Ni(1) atoms are linked via the azobipy molecules to form positively charged polymeric chains extended along the crystallographic *c* axis. The $btdc^{2-}$ anions serve as counterions. As a result, the $[Ni(azobipy)(H_2O)_4]^+$ chains form positively charged layers parallel to the *ac* plane and alternating with negatively charged layers consisting of the $Btdc^{2-}$ anions, thus providing the total neutral charge of the crystalline compound (Fig. 2b).

The XRD data for the powdered samples of compounds **I** and **II** correspond completely to the theoretically calculated diffraction patterns and confirm the phase purity of the synthesized compounds (Fig. 3). According to the TG data, compound **I** is stable to $T \approx$ 100°C, and then a slight mass loss (~8%) is observed associated with the removal of two coordinated water molecules. The weight of the coordination polymer remains unchanged up to $T \approx$ 340°C, after which thermolysis occurs. Compound **II** has the mass loss step (~12%) in a range of 140–180°C also related to the removal of four coordinated water molecules. The coordination polymer decomposes gradually at the temperature higher than 230°C (Fig. 4).

The IR spectrum of compound **I** exhibits bands characteristic of bending out-of-plane vibrations of the C–H bond at 777 cm^{-1} and bands of stretching symmetric and asymmetric vibrations of the C=O bond in the carboxylate groups at 1372 and 1547 cm^{-1}, respectively. The broad band at 3391 cm^{-1} is assigned to stretching vibrations of the O–H bond in the water molecule. The IR spectrum of compound **II** contains a band at 781 cm^{-1} attributed to bending out-of-plane vibrations of the C–H bond and bands characteristic of stretching symmetric and asymmetric vibrations of the C=O bond in the carboxylate groups at 1439 and 1564 cm^{-1}, respectively. A broad medium-intensity

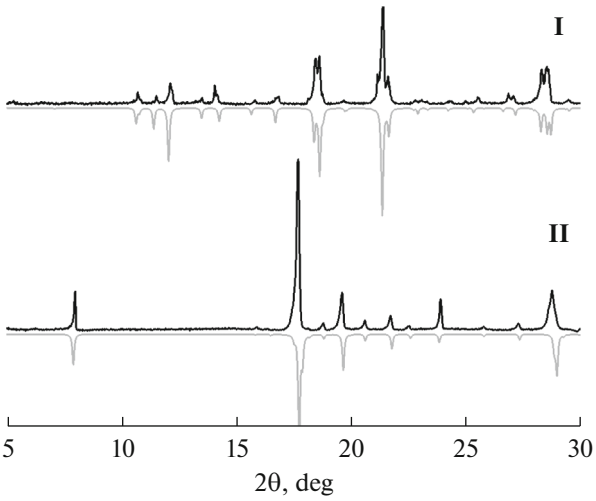

Fig. 3. Comparison of the (black) experimental and (gray) simulated powder diffraction patterns for compounds **I** and **II**.

band at 3291 cm^{-1} corresponds to stretching vibrations of the O–H bond in the water molecule.

The temperature dependences of the molar magnetic susceptibility ($\chi_p(T)$) of compound **I** were measured in a range of 1.77–300 K in the magnetic fields up to 10 kOe. The magnetic susceptibility of the MOF increased gradually with decreasing temperature to a minimum available temperature of 1.77 K, which is quite expected for a paramagnetic compound containing Ni^{2+} ions. After the diamagnetic contribution χ_d, which was calculated using Pascal's additive scheme, was subtracted from the total magnetic susceptibility, the remained paramagnetic component $\chi_p(T)$ was put on the plot as $1/\chi_p$ in the temperature dependence (Fig. 5). The $1/\chi_p(T)$ curve is close to linear nearly in the whole temperature range following the Curie–Weiss paramagnetic dependence $\chi_p(T) = N_A\mu_{eff}^2/3k_B(T-\theta)$ with $\theta \approx 1$–1.5 K The calculated value of μ_{eff} for compound **I** is 3.08 μ_B at 300 K, which is close to the spin-only value (2.83 μ_B) for the isolated high-spin Ni^{2+} ion with $S = 1$. An excess is caused by the contribution of the orbital moment to the magnetic moment of the nickel ion. A sharp decrease in μ_{eff} at the temperatures $T < 10$ K can be related to both the ion level splitting in the zero field expected for the Ni^{2+} ions with the spin $S = 1$ and a weak antiferromagnetic interaction between the ions. The dipole-dipole mechanism of the interionic interaction is next in significance after the exchange mechanism and exerts no determining effect in this case. The dipole-dipole interaction has a characteristic scale of energies $(g\mu_B)^2/r^3$ (r is the distance between the magnetic ions), which is ten times lower than the observed values of θ for the Ni^{2+} ions with $S = 1$ at the distances observed

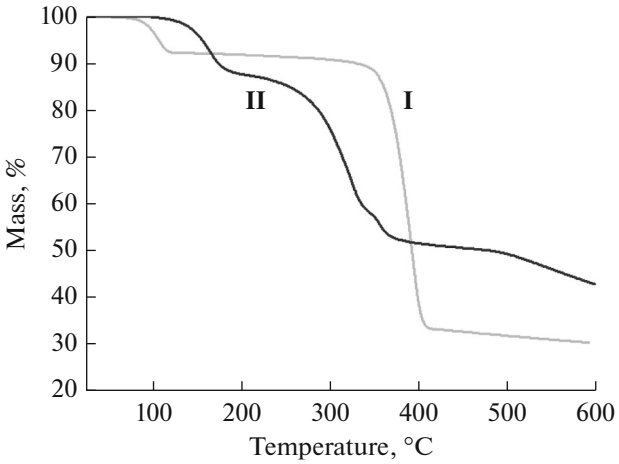

Fig. 4. TG curves for compounds (gray) **I** and (black) **II**.

in the MOF structure. Attempts of numerical description of the temperature dependence of μ_{eff} using the described approaches [18] showed that good agreement with experiment can be obtained only with allowance for both factors: splitting in the zero field and antiferromagnetic interaction. The results of approximation with the splitting factor $D/k_B \approx 4.8$ K and exchange intermolecular interaction $zJ \approx -0.16$ K, where z is the magnetic coordination number of Ni^{2+} ions, are shown by thin solid line in Fig. 5. The obtained value of D is characteristic of the Ni(II) complexes [18].

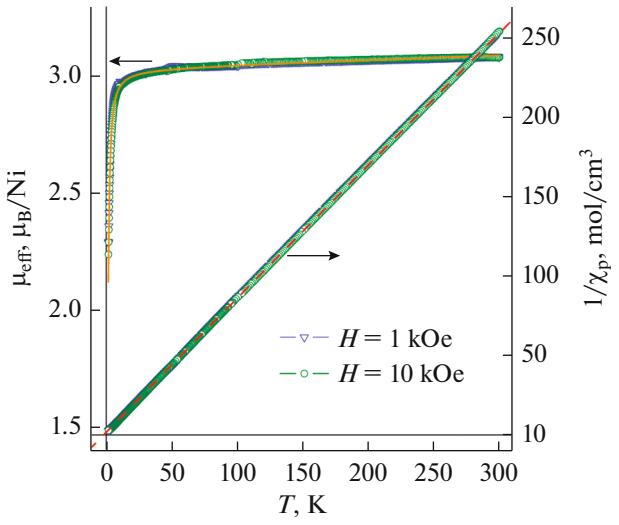

Fig. 5. Temperature dependences of $1/\chi_p$ and μ_{eff} per nickel ion for compound **I**. Magnetic field H = 1 and 10 kOe. Dashed line shows the formal description of the $1/\chi_p(T)$ curve by the Curie–Weiss dependence, and thin solid line shows the results of approximation of the $\mu_{eff}(T)$ dependence taking into account the splitting of the Ni^{2+} ion levels in the zero field and interionic exchange interaction.

The exchange interaction mechanisms in compound **I** are not evident. Inside the layer the paramagnetic centers are separated by long $btdc^{2-}$ and bipy organic ligands at distances of 14.9 and 11.3 Å, respectively, which makes impossible the exchange interaction between the Ni^{2+} ions within one layer. However, since MOF **I** is mutually intergrown, the distance between the Ni^{2+} ions of different layers shortens to 6.9 Å, which results, most likely, in the formation of routes for the weak antiferromagnetic interaction.

Thus, two new MOF based on Ni^{2+} ions were synthesized and completely characterized. The magnetic susceptibility and effective magnetic moment were measured for compound **I**.

FUNDING

This work was supported by the Russian Science Foundation, project no. 18-13-00203 (https://rscf.ru/project/18-13-00203/).

CONFLICT OF INTEREST

The authors declare that they have no conflicts of interest.

REFERENCES

1. Zhou, H.-C. and Kitagawa, S., *Chem. Soc. Rev.*, 2014, vol. 43, p. 5415.
2. Yuan, S., Feng, L., Wang, K., et al., *Adv. Mater.*, 2018, p. 1704303.
3. Schneemann, A., Bon, V., Schwedler, I., et al., *Chem. Soc. Rev.*, 2014, vol. 43, p. 6062.
4. Stock, N. and Biswas, S., *Chem. Rev.*, 2012, vol. 112, p. 933.
5. Demakov, P.A., Volynkin, S.S., Samsonenko, D.G., et al., Molecules, 2020, vol. 25, p. 4396.
6. Bolotov, V.A., Kovalenko, K.A., Samsonenko, D.G., et al., *Inorg. Chem.*, 2018, vol. 57, p. 5074.
7. Lysova, A.A., Samsonenko, D.G., Dorovatovskii, P.V., et al., *J. Am. Chem. Soc.*, 2019, vol. 141, p. 17260.
8. Hua, C. and D'Alessandro, D.M., *Cryst. Growth Des.*, 2017, vol. 17, p. 6262.
9. Zhao, J., Shi, X., Li, G., et al., *Inorg. Chim. Acta*, 2012, vol. 383, p. 185.
10. Ding, B., Hua, C., Kepert, C., et al., *Chem. Sci.*, 2019, vol. 10, p. 1392.
11. Dubskikh, V.A., Lysova, A.A., Samsonenko, D.G., et al., *Molecules*, 2021, vol. 26, p. 1269.
12. Demessence, A., Mesbah, A., Francois, M., et al., *Eur. J. Inorg. Chem.*, 2009, vol. 25, p. 3713.
13. Lu, K., Ma, D.-Y., and Sakiyama, H., *Inorg. Chem.* Commun., 2018, vol. 91, p. 39.
14. Alexander, D.S. and Robert, L.L., *Z. Anorg. Allg. Chem.*, 2016, vol. 642, p. 966.
15. Yeşilel O.Z., İlker İ., Şahin E., *J. Inorg. Organomet. Polym. Mater.*, 2011, vol. 21, p. 103.
16. Dong, J.-L., Zhu, P.-Y., Du, J.-Q., et al., *RSC Adv.*, 2019, vol. 9, p. 17560.
17. Dubskikh, V.A., Lysova, A.A., Samsonenko, D.G., et al., *J. Struct. Chem.*, 2020, vol. 61, p. 1800.
18. Boča, R., *Coord. Chem. Rev.*, 2004, vol. 248, p. 757.
19. Kabsch, W., *Acta Crystallogr., Sect. D: Biol. Crystallogr.*, 2010, vol. 66, p. 125.
20. *CrysAlisPro Software System. Version 1.171.40.84a*, 2020.
21. Sheldrick, G.M., *Acta Crystallogr., Sect. A: Found. Adv.*, 2015, vol. 71, p. 3.
22. Sheldrick, G.M., Acta Crystallogr., *Sect. C: Struct. Chem.,* 2020, vol. 71, p. 3.
23. Batten, S.R. and Robson, R., *Angew. Chem., Int. Ed. Engl.*, 1998, vol. 37, p. 1460.
24. Wang, K., Lv, B., and Wang, Z., *Dalton Trans.*, 2020, vol. 49, p. 411.
25. Verma, G., Butikofer, S., Kumar, S., et al., *ACS Appl. Mater. Interfaces*, 2019, vol. 12, p. 18715.

Translated by E. Yablonskaya